NANO LETTERS

2008
Vol. 8, No. 4
1202-1206

Isolation of Discrete Nanoparticle−DNA Conjugates for Plasmonic Applications

Shelley A. Claridge, Huiyang W. Liang, S. Roger Basu, Jean M. J. Fréchet,* and A. Paul Alivisatos*

Department of Chemistry, Berkeley, California 94720, and E. O. Lawrence Berkeley National Laboratory, Division of Materials Science, Berkeley, California 94720

Received January 21, 2008; Revised Manuscript Received February 16, 2008

ABSTRACT

Discrete DNA−gold nanoparticle conjugates with DNA lengths as short as 15 bases for both 5 and 20 nm gold particles have been purified by anion-exchange HPLC. Conjugates comprising short DNA (<40 bases) and large gold particles (≥20 nm) are difficult to purify by other means and are potential substrates for plasmon coupling experiments. Conjugate purity is demonstrated by hybridizing complementary conjugates to form discrete structures, which are visualized by TEM.

DNA−nanocrystal conjugates have proven to be an important addition to the arsenal for addressing many emerging challenges of nanoscience.[1–3] Gold and quantum dot[4] conjugates have been used extensively as biomolecular markers. Additionally, DNA base pairing has directed the self-assembly of discrete groupings and arrays of inorganic nanocrystals,[5,6] which may ultimately provide a route to self-assembled nanoscale electronic devices and memory components. Recently, plasmon coupling between gold nanoparticles conjugated to DNA has also been developed as a molecular ruler capable of detecting subnanometer distance changes over length and time scales inaccessible via fluorescence resonance energy transfer (FRET) measurements.[7,8]

For many of these applications, it is desirable to obtain nanocrystals functionalized with discrete numbers of DNA strands. For instance, hybridization of a mixture of two cDNA−gold monoconjugates will result in the formation of DNA−gold dimers,[9] whereas hybridizing polyconjugates results in formation of a network solid.[10] Thus, control over DNA-mediated assembly of complex inorganic nanostructures depends crucially upon the ability to isolate discrete DNA−gold building blocks in which the number of DNA strands is controlled.

Plasmon coupling experiments place substantial additional constraints on the conjugates.[7,8] In such experiments, the scattering intensity of a pair of nanoparticles depends on both the particle radius (R) as R^6 and the interparticle distance (R_P) as $1/R_P^6$.[11] For good plasmon coupling efficiency, noble metal nanoparticles at least 20 nm in diameter are required, with an interparticle distance less than or equal to the diameter of the particles. Consequently, it is desirable to use a DNA spacer that is short relative to the diameter of the nanoparticle, resulting in a small interparticle distance.

Although DNA−gold monoconjugates are routinely used by a variety of researchers, isolating nanocrystals functionalized with discrete numbers of short (<40 base) DNA strands has proven difficult. Separations are often carried out by agarose gel electrophoresis in which both the size of the nanoparticle and the length of the attached DNA are important, meaning that even longer DNA strands must be utilized to achieve adequate resolution for larger particles.[9,12] Other separation methods have been successfully used to purify nanoparticles bound to short DNA,[13–15] but to date these have been restricted to very small particles (≤10 nm), which have limited utility for plasmonic applications.

High-performance liquid chromatography (HPLC) and size-exclusion chromatography (SEC) are techniques that offer high resolving power and have been successfully used by other researchers to measure size distributions in samples of unconjugated nanoparticles,[16–20] and to purify nanoparticle−protein polyconjugates from unconjugated protein.[21] Here we investigate the use of anion exchange HPLC, a technique popular for purification of short, single-stranded DNA, in order to isolate nanocrystals functionalized with discrete numbers of short DNA strands.

Anion exchange is a form of HPLC in which the stationary phase is functionalized with cationic (usually quaternary ammonium) functional groups. The cationic surface strongly binds anions, in particular polyanionic molecules such as DNA. Analytes are eluted by increasing the salt concentration of the mobile phase until equilibrium favors release of the analyte from the stationary phase. AE-HPLC has been

* Corresponding authors. E-mail: frechet@berkeley.edu (J.M.J.F.); alivis@berkeley.edu (A.P.A.). Telephone: (510) 643-3077 (J.M.J.F.); (510) 643-7371 (A.P.A.). Fax: (510) 643-3079 (J.M.J.F.); (510) 642-6911 (A.P.A.).

10.1021/nl0802032 CCC: $40.75
Published on Web 03/11/2008

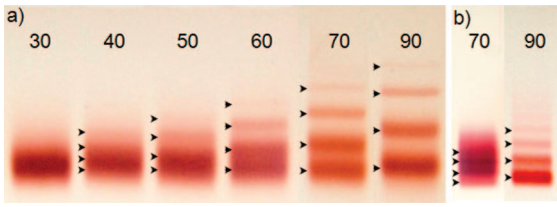

Figure 1. Electrophoretic analysis of gold conjugated to thiolated DNA of varying lengths. (a) 5 nm gold particles are conjugated to polyT DNA 30–90 bases in length. Black arrowheads indicate visible bands as a guide to the eye. (b) 20 nm gold particles conjugated to 70- and 90-base polyT DNA.

particularly successful in separations of short, single-stranded DNA, giving single-base resolution up to approximately 60 bases.[22]

Agarose gel electrophoresis has been widely used to purify gold nanocrystals conjugated to controlled numbers of DNA strands. When DNA−gold conjugate structures are analyzed by agarose gel electrophoresis, they give discrete bands corresponding to structures with increasing numbers of DNA strands.[12] For a given gel percentage, greater separation is observed for long DNA strands than for short strands. Figure 1 demonstrates this effect. When thiolated poly(T) DNA was conjugated to 5 nm gold particles and analyzed in a 3% agarose gel, bands were visible (although not well-resolved) for DNA as short as 40 bases. However, when the same DNA was conjugated to 20 nm AuNP, bands were only clearly visible for DNA at least 70 bases in length.

Aliquots of 5 and 20 nm conjugates were then analyzed by AE-HPLC. In a typical analysis, 100 μL of nanoparticle conjugate solution (about 300 pmol of 5 nm particles or 3 pmol of 20 nm particles) was injected with an aqueous mobile phase incorporating 40 mM NaCl to encourage strong binding of polyanions (such as DNA) to the stationary phase. After 3 min at the low salt concentration, the NaCl concentration was raised from 40 to 900 mM over 20 min. Gold elution was observed by monitoring the UV–vis absorbance at the gold plasmon peak of 520 nm vs a reference wavelength of 850 nm, at which gold colloid has very low absorbance, and visually confirmed by the presence of the characteristic red color of the colloid in collected fractions. A representative set of HPLC traces are shown in Figure 2. As expected, each sample exhibits a broad peak eluting at a low ionic strength, corresponding to unconjugated gold. Small variations in these peaks were sometimes observed due to slight differences in the completeness of the neutral poly(ethylene glycol) (PEG) ligand shell passivating the particles (see Supporting Information). The traces in Figure 2 are normalized to the position of the unconjugated gold peak in order to observe the effect of increasing DNA length.

The second peak eluted at an ionic strength dependent upon the length of DNA oligomer conjugated to the gold particle. As in the electrophoretic purification, the separation between unconjugated (first peak) and monoconjugated (second peak) gold increased with increasing DNA length. Disconjugate (third peak) was also separated from monoconjugate, although the separation was not as pronounced

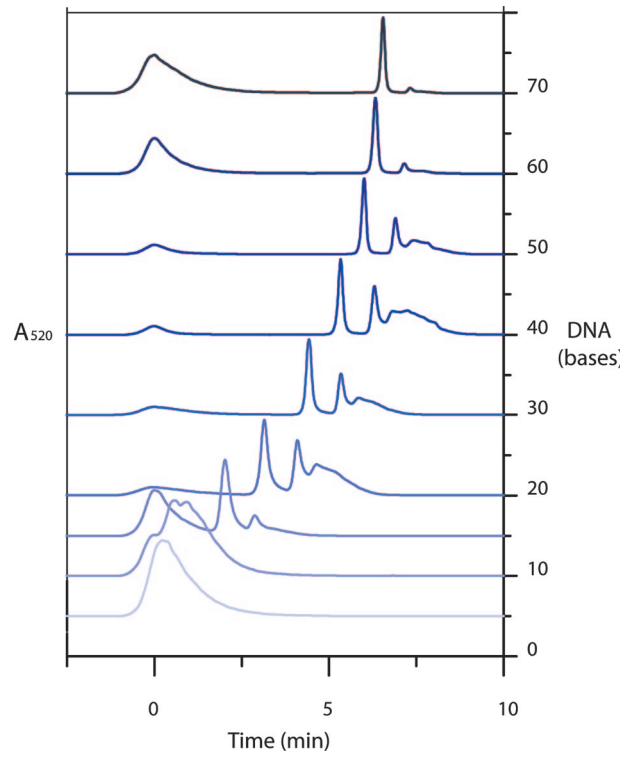

Figure 2. Elution profiles of varying lengths of polyT DNA conjugated to 20 nm AuNP. Leftmost peak is unconjugated gold. Monoconjugate peak migrates to longer retention times as DNA length is increased, with near-baseline separation achieved for monoconjugates of 15-base DNA.

as that between unconjugated gold and monoconjugate. Near-baseline resolution was achieved for 15-base conjugates in the HPLC, while for DNA shorter than 15 bases, peaks were not well resolved. It should be noted that DNA retention in AE-HPLC is known to be slightly sequence-dependent;[23] in these experiments, the use of polyT sequences ensures that differences in retention can be attributed solely to DNA length.

It should also be noted that AE-HPLC is often superior to gel electrophoresis as a DNA−gold conjugate purification method, even for cases in which discrete bands are clearly visible in a gel. A direct comparison of the two methods is shown in Figure 3 for 5 nm AuNP conjugated to 70-base DNA. Although bands in the gel appear well-separated, optical density analysis (Figure 3a, lower frame) demonstrates that the monoconjugate band has significant overlap with both the unconjugated gold and the diconjugate. HPLC purification of the same type of conjugates is shown in Figure 3b: here, baseline resolution is achieved for the first three peaks, indicating that high-purity monoconjugates can be recovered. Typical monoconjugate yields from a 100 μL injection were 30–50 pmol for 5 nm particles and 0.3–0.5 pmol for 20 nm particles, similar to quantities extracted from an 8-well agarose gel, making AE-HPLC a viable preparative technique for DNA−Au conjugate self-assembly experiments.

Although monoconjugates can clearly be separated from unconjugated gold and diconjugate using AE-HPLC, the conjugates should also be separated from any excess uncon-

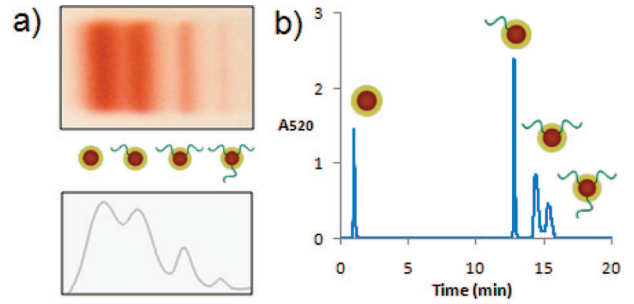

Figure 3. Comparison of agarose gel and AE-HPLC purification of 70-base polyT DNA conjugated to 5 nm AuNP. (a) Gel purification of conjugates. Although four distinct bands are visible, a lane trace produced by optical density analysis shows monoconjugate overlaps with both unconjugated gold and diconjugate. (b) When the same structures are purified by AE-HPLC, baseline resolution is observed for the first three peaks.

jugated DNA in order to ensure that no further conjugation can take place after purification.

To quantify DNA retention, free thiolated poly(T) DNA was analyzed using the same gradient applied to the conjugates. Elution was observed by monitoring the UV–vis absorption at the DNA absorption peak of 260 nm vs a reference wavelength of 360 nm at which DNA does not absorb strongly. In general, a single large peak was observed, although occasionally a very small secondary peak (area <5% of primary peak area) was also observed at slightly lower ionic strength, suggestive of a small amount of DNA degradation. The position of the primary peak was used in plotting DNA retention (Figure 4a).

Interestingly, both mono- and diconjugates elute at lower ionic strength (shorter times) than the free thiolated DNA of the same length. Attaching the DNA to a gold nanoparticle coated with neutral ligands is expected to decrease retention of the DNA because the ligand shell around the gold nanoparticle will interfere with binding of the DNA bases proximal to the nanoparticle. It is also not surprising that addition of a second DNA strand does not impact retention as much as the first, since the effect of additional DNA bases binding the column decreases sharply after the first 30 bases (see DNA curve in Figure 4a). Additionally, it is expected that the DNA strands are distributed on the surface of the nanoparticle, which may prevent the second strand from binding as completely as the first.

Surface passivation of the nanoparticle is also key in determining the retention behavior of conjugate structures (Figure 4b). Passivation with neutral thiolated PEG results in unconjugated gold eluting at very low ionic strengths, whereas use of carboxy-terminated (anionic) PEG results in much stronger retention of unconjugated gold because the ligands on the surface of the gold can also bind the column. Differences can be seen in the gold and monoconjugate elution for passivation with short neutral vs long neutral PEG molecules, presumably because the thicker ligand shell created by longer PEG molecules slightly reduces the number of DNA bases free to bind the column. Because the Debye screening length in the mobile phase ranges from 1.24 nm at the beginning of the run to 0.34 nm at the end of the run,

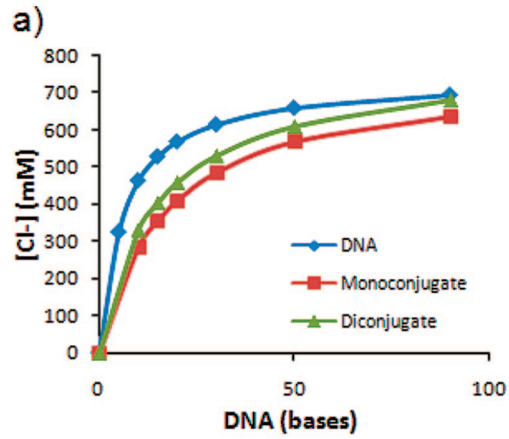

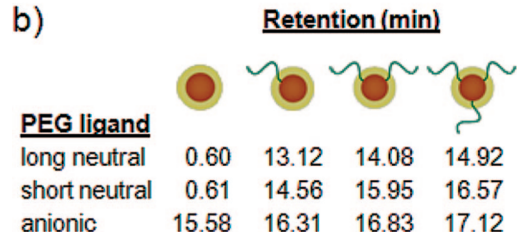

Figure 4. (a) AE-HPLC retention of free DNA compared with DNA conjugated to 5 nm AuNP. At all DNA lengths, free DNA is retained more strongly than 5 nm AuNP conjugated to one or two strands of the same DNA. Peak width at half the maximum value is approximately 4 mM for DNA and 20 mM for mono- and diconjugate. (b) Ligand used to passivate gold surface plays an important role in conjugate retention, although in each case, increasing numbers of DNA strands correlate with increased retention.

it is also possible that charges on the gold surface under the PEG ligands could play a small role in retention behavior. These charges could arise either from the gold particle synthesis procedure or from a small number of residual anionic phosphine ligands left after the PEG ligands are exchanged onto the particles.

To demonstrate that HPLC-purified conjugates are good substrates for self-assembly, 20 nm gold particles discretely functionalized with one, two, or three strands of DNA were isolated and hybridized with complementary conjugates of 5 nm gold. Hybrid structures were visualized by TEM.

Typically when TEM images are used to characterize DNA-templated self-assembly of nanoparticles, interparticle distance can be used to infer the length of the DNA linker, which is not itself visible under the electron beam. However, the increased forces acting on larger nanoparticles as the sample dries on the TEM grid can be sufficient to bend the DNA linker (Figure 6), so structures were also assembled in which a central, discretely functionalized 20 nm particle bearing one (Figure 5a), two (Figure 5b), or three (Figure 5c) 60-base DNA strands was hybridized to the appropriate number of monofunctional 5 nm particles. Although some drying-induced DNA bending was observed in these structures as well (Figure 5b inset), enough hybrids adopt an extended conformation to make a convincing argument for DNA-mediated assembly rather than nonspecific aggregation.

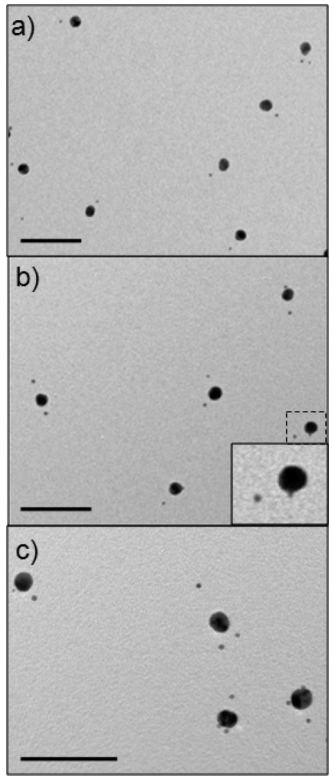

Figure 5. TEM characterization of hybridized 20 nm/5 nm conjugate structures: (a) 20 nm monoconjugates hybridized with complementary 5 nm monoconjugates, (b) 20 nm diconjugates hybridized with 5 nm monoconjugates, and (c) 20 nm triconjugates hybridized with 5 nm monoconjugates. Inset in (b) shows that structures may collapse during drying on the TEM grid, pulling one or more of the 5 nm particles close to the 20 nm particle. Scale bar = 100 nm.

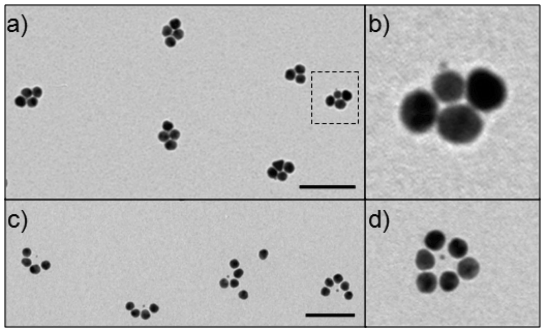

Figure 6. TEM characterization of hybridized 20 nm/5 nm conjugate structures: (a) 20 nm monoconjugates hybridized with complementary 5 nm tetraconjugates, (b) closeup of boxed structure from (a), showing that a single 5 nm particle is part of the assembly as expected. (c) 20 nm/5 nm assemblies demonstrating local differences in dried assembly morphology. (d) Higher-order 20 nm/5 nm assembly with ringlike morphology. Scale bar = 100 nm.

These experiments demonstrate that not only mono- but also di- and triconjugates can be isolated in sufficient purity for use as self-assembly substrates.

Radial assemblies were also formed in which 5 nm polyconjugates were hybridized to 20 nm monoconjugates. In a large percentage of structures, the 20 nm particles are pulled into contact with each other during drying (Figure 6a). This can obscure the 5 nm polyconjugated hub, however, the 5 nm particle is usually visible when the structure is viewed more closely (Figure 6b). Drying conditions are believed to play an important role in the morphology of 20 nm multiparticle assemblies. For instance, parts a and c of Figure 6 are assembled using conjugates prepared from the same DNA. Importantly, this suggests that the 20 nm particles are not aggregated in solution, a key prerequisite for utilizing the assemblies in plasmonic experiments.

In conclusion, we have successfully isolated discrete DNA−gold conjugates suitable for plasmonic applications, composed of a large gold nanoparticle attached to controlled numbers of short DNA strands. The anion-exchange purification method used in isolating these conjugates is also an improvement on the existing gel electrophoresis purification method for other DNA gold conjugates (e.g., small nanoparticle attached to longer DNA) routinely used for nanoscale self-assembly experiments. Ongoing experiments seek to determine the size limits of this new method. The large size of the column packing material (approximately 13 μm spheres) results in interstitial spaces quite large in comparison to the conjugates, thus it is expected that similar methodology may be applied to much larger particles. However, the increased sensitivity of larger nanoparticles to high salt concentrations will require careful optimization of the nanoparticle surface passivation conditions. We also plan to leverage the new range of discrete nanoparticle conjugates described here to develop an expanded set of plasmon ruler measurements.

Acknowledgment. This work was supported by the Director, Office of Science, Office of Basic Energy Sciences, Materials Sciences and Engineering Division of the U.S. Dept. of Energy under contract no. DE-AC02-05CH11231. S.A.C. gratefully acknowledges an NSF-IGERT Predoctoral Fellowship.

Supporting Information Available: Materials and Methods, unnormalized 20 nm polyT HPLC traces. This material is available free of charge via the Internet at http://pubs.acs.org.

References

(1) Katz, E.; Willner, I. *Angew. Chem., Int. Ed.* **2004**, *43* (45), 6042–6108.
(2) Niemeyer, C. M. *Angew. Chem., Int. Ed.* **2001**, *40* (22), 4128–4158.
(3) Alivisatos, A. P.; Johnsson, K. P.; Peng, X. G.; Wilson, T. E.; Loweth, C. J.; Bruchez, M. P.; Schultz, P. G. *Nature* **1996**, *382* (6592), 609–611.
(4) Fu, A. H.; Gu, W. W.; Larabell, C.; Alivisatos, A. P. *Curr. Opin. Neurobiol.* **2005**, *15* (5), 568–575.
(5) Zheng, J. W.; Constantinou, P. E.; Micheel, C.; Alivisatos, A. P.; Kiehl, R. A.; Seeman, N. C. *Nano Lett.* **2006**, *6* (7), 1502–1504.
(6) Claridge, S. A.; Goh, S. L.; Frechet, J. M. J.; Williams, S. C.; Micheel, C. M.; Alivisatos, A. P. *Chem. Mater.* **2005**, *17* (7), 1628–1635.
(7) Sonnichsen, C.; Reinhard, B. M.; Liphardt, J.; Alivisatos, A. P. *Nat. Biotechnol.* **2005**, *23* (6), 741–745.
(8) Reinhard, B. M.; Sheikholeslami, S.; Mastroianni, A.; Alivisatos, A. P.; Liphardt, J. *Proc. Natl. Acad. Sci. U.S.A.* **2007**, *104* (8), 2667–2672.
(9) Zanchet, D.; Micheel, C. M.; Parak, W. J.; Gerion, D.; Williams, S. C.; Alivisatos, A. P. *J. Phys. Chem. B* **2002**, *106* (45), 11758–11763.
(10) Elghanian, R.; Storhoff, J. J.; Mucic, R. C.; Letsinger, R. L.; Mirkin, C. A. *Science* **1997**, *277* (5329), 1078–1081.
(11) Kreibig, U. V. M. *Optical Properties of Metal Clusters*; Springer: Berlin, 1995.

(12) Zanchet, D.; Micheel, C. M.; Parak, W. J.; Gerion, D.; Alivisatos, A. P. *Nano Lett.* **2001**, *1* (1), 32–35.
(13) Ackerson, C. J.; Sykes, M. T.; Kornberg, R. D. *Proc. Natl. Acad. Sci. U.S.A.* **2005**, *102* (38), 13383–13385.
(14) Qin, W. J.; Yung, L. Y. L. *Langmuir* **2005**, *21* (24), 11330–11334.
(15) Jhaveri, S. D.; Foos, E. E.; Lowy, D. A.; Chang, E. L.; Snow, A. W.; Ancona, M. G. *Nano Lett.* **2004**, *4* (4), 737–740.
(16) Al-Somali, A. M.; Krueger, K. M.; Falkner, J. C.; Colvin, V. L. *Anal. Chem.* **2004**, *76* (19), 5903–5910.
(17) Krueger, K. M.; Al-Somali, A. M.; Falkner, J. C.; Colvin, V. L. *Anal. Chem.* **2005**, *77* (11), 3511–3515.
(18) Wilcoxon, J. P.; Provencio, P. P. *J. Phys. Chem. B* **2005**, *109* (28), 13461–13471.
(19) Wilcoxon, J. P.; Martin, J. E.; Provencio, P. *Langmuir* **2000**, *16* (25), 9912–9920.
(20) Choi, M. M. F.; Douglas, A. D.; Murray, R. W. *Anal. Chem.* **2006**, *78* (8), 2779–2785.
(21) Wang, S. P.; Mamedova, N.; Kotov, N. A.; Chen, W.; Studer, J. *Nano Lett.* **2002**, *2* (8), 817–822.
(22) Weiss, J. *Handbook of Ion Chromatography*; Wiley: Darmstadt, 2004; Vol. 1.
(23) Yamamoto, S.; Nakamura, M.; Tarmann, C.; Jungbauer, A. *J. Chromatogr., A* **2007**, *1144* (1), 155–160.

NL0802032